Human Pathology 143 (2024) 50–61

Contents lists available at ScienceDirect

Human Pathology

journal homepage: www.elsevier.com/locate/humpath

Gastric metaplasia as a precursor of nonconventional dysplasia in inflammatory bowel disease

Eva Musulen [a,b,*], Míriam Gené [c,d], Míriam Cuatrecasas [e,f], Irene Amat [g], Jesús Alberto Veiga [h], María Jesús Fernández-Aceñero [i], Victòria Fusté Chimisana [j], Jordi Tarragona [k], Ismael Jurado [l], Rebeca Fernández-Victoria [m], Carolina Martínez-Ciarpaglini [n], Cristina Alenda González [o], Carlos Zac [p], María Teresa Fernández-Figueras [a,q], Manel Esteller [b,r,s,t]

[a] Pathology Department, Hospital Universitari General de Catalunya-Grupo QuironSalud, 08915 Sant Cugat Del Vallès, Barcelona, Spain
[b] Institut de Recerca Contra La Leucèmia Josep Carreras (IJC), 08916 Badalona, Barcelona, Spain
[c] Pathology Department, Hospital Universitari Joan XXIII, 43005 Tarragona, Spain
[d] Surgery Department, Programme of Surgery and Morphological Sciences, Universitat Autònoma de Barcelona (UAB), 08193 Cerdanyola Del Vallès, Spain
[e] Pathology Department, Hospital Clínic, 08036 Barcelona, Spain
[f] Department of Basic Clinical Practice, University of Barcelona (UB), 08036 Barcelona, Spain
[g] Pathology Department, Complejo Hospitalario de Navarra, 31008 Navarra, Spain
[h] Pathology Department, Complejo Hospitalario Universitario de Ferrol, 15405 Ferrol, Spain
[i] Pathology Department, Hospital Clínico San Carlos, 28040 Madrid, Spain
[j] Pathology Department, Hospital de La Santa Creu I Sant Pau, 08025 Barcelona, Spain
[k] Pathology Department, Hospital Universitari Arnau de Vilanova, 25198 Lleida, Spain
[l] Pathology Department, Consorci Sanitari de Terrassa, 08227 Terrassa, Spain
[m] Pathology Department, Hospital Álvaro Cunqueiro, 36312 Vigo, Spain
[n] Pathology Department, Hospital Clínico Universitario de Valencia, INCLIVA- Instituto de Investigación Sanitaria, Universidad de Valencia, 46010 Valencia, Spain
[o] Pathology Department, Hospital General Universitario Dr. Balmis, Instituto de Investigación Sanitaria y Biomédica de Alicante (ISABIAL), 031010 Alicante, Spain
[p] Pathology Department, Hospital Universitari I Politècnic La Fe, 46026 Valencia, Spain
[q] School of Medicine, Campus Sant Cugat Del Vallès, Universitat Internacional de Catalunya (UIC), 08917 Sant Cugat Del Vallès, Spain
[r] Institució Catalana de Recerca I Estudis Avançats (ICREA), 08010 Barcelona, Spain
[s] Faculty of Medicine and Health Sciences, Department of Physiological Sciences, Universitat de Barcelona (UB), 08007 Barcelona, Spain
[t] Centro de Investigación Biomédica en Red Cáncer (CIBERONC), 28029 Madrid, Spain

ARTICLE INFO

Keywords:
Gastric metaplasia
Nonconventional dysplasia
Conventional dysplasia
Inflammatory bowel disease
CRC serrated pathway

ABSTRACT

Gastric metaplasia in colonic mucosa with inflammatory bowel disease (IBD) develops as an adaptation mechanism. The association between gastric metaplasia and nonconventional and/or conventional dysplasia as precursors of colitis-associated colorectal cancer is unknown. To address this question, we retrospectively reviewed a series of 33 IBD colectomies to identify gastric metaplasia in 76 precursor lesions.

We obtained 61 nonconventional and 15 conventional dysplasias. Among nonconventional dysplasia, 31 (50.8 %) were low-grade (LGD), 4 (6.5 %) were high-grade (HGD), 9 (14.8 %) had both LGD and HGD, and 17 (27.9 %) had no dysplasia (ND), while 14 (93 %) conventional dysplasias had LGD, and 1 (7 %) had LGD and HGD.

Gastric metaplasia was assessed by concomitant immunoexpression of MUC5AC and loss of CDX2 staining. Expression of a p53-mut pattern was considered as a surrogate for gene mutation, and complete loss of MLH1 staining as presence of *MLH1* hypermethylation.

In nonconventional dysplasia, MUC5AC immunoexpression decreased as the degree of dysplasia increased, being 78 % in LGD and 39 % in HGD ($p = 0.006$). CDX2 was lost in epithelial glands with high expression of MUC5AC ($p < 0.001$). The p53-mut pattern was observed in 77 % HGD, 45 % LGD, and in 6 % with ND ($p < 0.001$). Neither nonconventional nor conventional dysplasia showed complete loss of MLH1 staining. Gastric metaplasia was also present in mucosa adjacent to nonconventional dysplasia with chronic changes or active

* Corresponding author. Hospital Universitari General de Catalunya-Grupo QuironSalud Pathology Department C/ Pedro i Pons, 1 08915 Sant Cugat del Vallès Barcelona, SpainInstitut de Recerca contra la Leucèmia Josep Carreras (IJC), Grup d'Epigenètica del Càncer, Josep Carreras Building, Ctra de Can Ruti, Camí de les Escoles, s/n, 08916 Badalona, Barcelona, Spain

E-mail addresses: emusulen@carrerasresearch.org, eva.musulen@quironsalud.es (E. Musulen).

https://doi.org/10.1016/j.humpath.2023.11.011
Received 24 July 2023; Received in revised form 18 October 2023; Accepted 17 November 2023
Available online 23 November 2023

inflammation. Our results show that gastric metaplasia appears in IBD-inflamed colon mucosa, it is the substrate of most nonconventional dysplasia and occurs prior to p53 alterations.

1. Introduction

Crohn's disease (CD) and ulcerative colitis (UC) are conditions with a 2- to 3-fold increased risk of colorectal cancer (CRC) [1,2] and colitis-associated colorectal cancer (CAC) is the main cause of death in long-standing inflammatory bowel disease (IBD) [3]. Certain factors such as severity of the disease, extensive involvement of the colon (pancolitis), young age at diagnosis, more than 8 years of disease, and the presence of extracolonic manifestations, especially primary sclerosing cholangitis, have been associated with a higher risk of malignancy [4,5]. In IBD, chronic inflammation inducing injury-repair processes and microbiota dysbiosis generate continuous stress on the colon mucosa. Repeated damage in extensive areas of the colon leads to the transformation of the mucosa into a cancerization field [6] with the appearance of multiple precursor lesions which may have no morphological dysplastic features, but that harbor molecular alterations capable of initiating CAC carcinogenesis [7].

To prevent the occurrence of CAC, surveillance colonoscopies are performed to identify dysplasia, traditionally considered the precursor lesion of CAC [8,9]. In 2017, Harzac et al. [10] described seven different categories which they termed *dysplasia* associated to IBD, and were named as follows: dysplasia with terminal epithelial differentiation, sessile serrated polyp/adenoma-like dysplasia, traditional serrated adenoma-like dysplasia, conventional adenoma-like dysplasia, hypermucinous dysplasia, goblet cell depleted dysplasia, and serrated dysplasia not otherwise specified (NOS). Currently, most of these entities are included under the designation of nonconventional dysplasia, to differentiate them from the conventional dysplasia, i.e., tubular adenoma (or tubular adenoma-like) and tubulovillous adenoma (or tubulovillous adenoma-like) [11]. Some of the above entities have been renamed, such as the former dysplasia with terminal epithelial differentiation by crypt cell atypia/dysplasia [12], and the serrated dysplasia NOS by serrated lesion NOS [11]. Other new categories have been recently recognized, such as the dysplasia with increased Paneth cell differentiation [11] and some new non-adenomatous lesions [13], and the serrated epithelial change has been redefined [14]. Moreover, there has been increasing interest in characterizing the molecular alterations of these recently described types of dysplasia to better understand the contribution of each entity to CAC carcinogenesis [7,12–19].

Gastric metaplasia has been identified as a substrate for the initiation of the serrated pathway of CRC, due to a multifactorial continuous injury of the right colon epithelium [20]. In addition, in the context of IBD, both foveolar and pseudopyloric gastric metaplasia can be seen. We have previously shown by analyzing a series of CAC and the surrounding colonic mucosa that gastric metaplasia occurs in colonic inflamed mucosa, it persists in chronic changes, and disappears with the acquisition of dysplasia and p53 mutations. Furthermore, we identified a subset of CRC in IBD related to the serrated pathway and characterized by the absence of mutated p53 pattern, microsatellite instability and MUC5AC expression [21]. Since the relationship between gastric metaplasia and nonconventional dysplasia as a precursor of CAC is unknown, we aimed to study a series of IBD colectomies to explore the presence of gastric metaplasia in nonconventional and conventional dysplasias.

2. Materials and methods

2.1. Patients and specimens

Thirty-three colectomies of IBD patients from 13 hospitals were retrospectively reviewed to identify precursor lesions of CAC. To characterize them, we used the following definitions: a) Goblet cell deficient dysplasia: flat, tubular lesion, with unequivocal dysplastic crypts characterized by complete or nearly-absence of goblet cells; b) Crypt cell atypia/dysplasia: flat lesion showing crypts with cells with round-to-oval, non-stratified nuclei with loss but not complete absence of goblet cells. The atypia can be located at the base of the crypt but does not affect the superficial epithelium; c) Dysplasia with increased Paneth cell differentiation: characterized by dysplastic crypts lined by hyperchromatic, mostly elongated nuclei with reduced goblet cells showing increased Paneth cell differentiation involving more than two contiguous crypts; e) Serrated epithelial change: flat or slightly elevated lesion with markedly distorted architecture and loss of crypt orientation, not perpendicularly aligned to the muscularis mucosae, and often chronic inflammation between the base of the crypt and the muscular mucosae; f) Hypermucinous dysplasia: villous or tubulovillous lesion with prominent mucinous differentiation involving more than 50 % of the lesion; g) Sessile serrated lesion-like: polypoid growth of crypts with prominent serration, base dilatation and horizontal growth along the muscularis mucosae; h) Traditional serrated adenoma-like: polypoid proliferation showing slit-like serration with tall columnar cells with intensely

Table 1
Clinicopathological features of IBD patients and adenocarcinomas.

	Crohn's disease (%)	Ulcerative colitis (%)	Total (%)	p value
Patients	9 (100)	24 (100)	33 (100)	
Age				
Mean years [range]	59.7 [32–82]	63.8 [30–85]	62.6 [30–85]	
Gender				0.137
Male	9 (100)	19 (79)	28 (85)	
Female	0	5 (21)	5 (15)	
IBD duration				0.408
Mean years [range]	15.4 [1-25]	12.5 [1-34]	14.8 [1-34]	
Concominant	2 (22.2)	2 (8)	4 (12.1)	
<8 years	1 (11.1)	7 (29)	8 (24.2)	
9–15 years	4 (44.4)	5 (21)	9 (27.3)	
16–20 years	1 (11.1)	6 (25)	7 (21.2)	
>21 years	1 (11.1)	4 (17)	5 (15.2)	
IBD activity				0.407
Active	5 (56)	17 (71)	22 (67)	
Quiescent	4 (44)	7 (29)	11 (33)	
Multifocal dysplasia				0.350
No	4 (44)	15 (62.5)	19 (58)	
Yes	5 (56)	9 (37.5)	14 (42)	
Type of dysplasia				0.924
Only NCD	6 (67)	15 (62.5)	21 (64)	
Only CD	2 (22)	5 (20.8)	7 (21)	
NCD and CD	1 (11)	4 (16.7)	5 (15)	
Concomitant adenocarcinoma				0.716
No	4 (44)	9 (37.5)	13 (39)	
Yes	5 (56)	15 (62.5)	20 (61)	
Adenocarcinoma per colectomy (n = 20)				0.278
1	5 (100)	12 (80)	17 (85)	
2	0	3 (20)	3 (15)	
Adenocarcinoma location (n = 23)				0.394
Right colon	3 (60)	4 (22)	7 (30.4)	
Left colon	1 (20)	6 (33)	7 (30.4)	
Rectum	0	3 (17)	3 (13)	
Colon	1 (20)	5 (28)	6 (26.1)	
Histology (n = 23)				0.620
NOS	5 (100)	13 (72.2)	18 (78.3)	
Mucinous	0	3 (16.7)	3 (13)	
Poorly differentiated	0	1 (5.6)	1 (4.3)	
Undifferentiated	0	1 (5.6)	1 (4.3)	

Table 2
Clinicopathological features of nonconventional and conventional dysplasia according to the type of IBD.

	Nonconventional dysplasia (n = 61)				Conventional dysplasia (n = 15)			
	Crohn's disease (n = 10)	Ulcerative colitis (n = 51)	Total (%)	p value	Crohn's disease (n = 6)	Ulcerative colitis (n = 9)	Total (%)	p value
Gender								
Male	10	43	53 (87)	0.332	6	9	15 (100)	
Female	0	8	8 (13)		0	0	0	
IBD duration				0.365				0.138
Concominant	1	4	5 (8.2)		5	2	7 (46.7)	
<8 years	2	8	10 (16.4)		0	1	1 (6.7)	
9–15 years	4	10	14 (23)		1	1	2 (13.3)	
16–20 years	1	22	23 (37.7)		0	4	4 (26.7)	
>21	2	7	9 (14.8)		0	1	1 (6.7)	
IBD activity				0.912				0.264
Active	8	40	48 (79)		1	4	5 (33)	
Quiescent	2	11	13 (21)		5	5	10 (67)	
Location of inflammation				0.000				0.003
Right colon	4	0	4 (6.5)		5	0	5 (33)	
Left colon	0	24	24 (39)		1	6	7 (47)	
Rectum	0	1	1 (1.5)		0	0	0	
Pancolitis	2	18	20 (33)		0	3	3 (20)	
NS	4	8	12 (20)		0	0	0	
Type of dysplasia								
Nonconventional dysplasia				0.455				
HM	2	12	14 (23.0)					
GCD	3	9	12 (19.7)					
SL NOS	2	7	9 (14.8)					
SSL-like	0	7	7 (11.5)					
CCA/D	0	7	7 (11.5)					
SEC	1	6	7 (11.5)					
TSA-like	2	2	4 (6.5)					
DPD	0	1	1 (1.5)					
Conventional dysplasia								0.398
TA-like					6	8	14 (93)	
TVA-like					0	1	1 (7)	
Dysplasia morphology				0.776				
Flat	5	28	33 (54)		0	0	0	
Polypoid	5	23	28 (46)		6	9	15 (100)	
Location of dysplasia				0.040				0.144
Right colon	4	10	14 (23)		4	1	5 (33)	
Left colon	2	8	10 (16.4)		1	3	4 (27)	
Rectum	0	17	17 (28)		0	2	2 (13)	
Colostomy	1	0	1 (1.5)		0	0	0	
NS	3	16	19 (31)		1	3	4 (27)	
Grade of dysplasia				0.186				0.398
LGD	8	23	31 (50.8)		6	8	14 (93)	
HGD	0	4	4 (6.6)		0	0	0	
LGD and HGD	0	9	9 (14.8)		0	1	1 (7)	
ND	2	15	17 (27.9)		0	0	0	
GM in type of dysplasia (n = 70)				0.097				0.1875
Yes	2	30	32 (46 %)		1	2	3 (19)	
No	8	30	38 (54 %)		5	8	13 (81)	
Adjacent mucosa to the dysplasia				0.205				0.114
Yes	5	36	41 (67)		6	6	12 (80)	
No	5	15	20 (33)		0	3	3 (20)	
Active inflammation	2	10	12 (29 %)		0	0	0	
Chronic inflammation/changes	2	20	22 (54 %)		2	0	2 (17 %)	
Normal	1	6	7 (17 %)		4	6	10 (83 %)	
GM in adjacent mucosa to the dysplasia (n = 41)				1000				
Yes	3	21	24 (58.5)		0	0	0	
No	2	15	17 (41.5)		6	6	12 (100)	
Active inflammation	1	7	8 (33.3)		0	0	0	
Chronic inflammation/changes	1	13	14 (58.3)		0	0	0	
Normal	1	1	2 (8.3)		0	0	0	
Concomitant adenocarcinoma				0.595				0.114
Yes	4	16	20 (33)		6	6	12 (80)	
No	6	35	41 (67)		0	3	3 (20)	

Abbreviations: NS, not specified; HM, hypermucinous; GCD, goblet cell deficient; SL NOS, serrated lesion not otherwise specified; CCA/D, crypt cell atypia/dysplasia; SEC, serrated epithelial change; SSL-like, sessile serrated lesion like; TSA-like, traditional serrated adenoma like; DPD, dysplasia with increased Paneth cell differentiation; TA-like, tubular adenoma like; TVA-like, tubulovillous adenoma like; LGD, low-grade dysplasia; HGD, high-grade dysplasia; ND, no dysplasia; GM, gastric metaplasia.

eosinophilic cytoplasm and ectopic crypt formation, frequently with low grade dysplasia (LGD); i) Serrated lesion not otherwise specified (serrated lesion NOS): those polypoid lesions without definite features of traditional serrated adenoma-like or sessile serrated lesion-like.

Histologic evaluation was performed separately by three expert pathologists in gastrointestinal pathology (M.G., M.C. and E.M.). Cases with discordant diagnoses were reviewed together to reach a consensus on the final diagnosis.

Information about the endoscopic appearance of the lesions was not available for all cases since the lesions were obtained from colectomies. Thus, those lesions that did not protrude more than half the thickness of the mucosa were considered flat. The rest were considered flat or polypoid by definition, such as serrated epithelial change as flat, or tubulovillous adenoma-like as polypoid.

2.2. Immunohistochemistry

Formalin-fixed, paraffin-embedded tissue sections were analyzed using standard immunohistochemistry (IHC) techniques. Immunostaining was performed automatically using a Ventana BenchMark ULTRA machine (Roche, Basel, Switzerland] for *anti*-p53 (clone DO-7, Ventana Medical Systems, Inc., 1910 E. Innovation Park Drive, Tucson, Arizona 85,755 USA) and *anti*-MUC5AC (clone MRQ-19, Ventana Medical Systems, Inc., 1910 E. Innovation Park Drive, Tucson, Arizona 85,755 USA), and a Bond-III machine (Leica Biosystems, Newcastle Upon Tyne, UK) for *anti*-CDX2 (clone EP25, Leica Biosystems, Newcastle Upon Tyne, UK) and *anti*-MLH1 (clone ES05, Leica Biosystems, Newcastle Upon Tyne, UK). An external positive control was included on each slide. Immunostaining was independently evaluated by three pathologists (M.G., M.C. and E.M.).

For the evaluation of p53 immunostaining we used the 3-level scores described by Köbel et al. [22]. Strong and intense p53 staining in all nuclei (overexpression pattern) and total absence of nuclear staining (null pattern) were considered as surrogates for *TP53* mutation (p53-mut pattern). Focal nuclear positivity with variable intensity was considered as normal or wild-type pattern (p53-wt pattern).

MUC5AC identified foveolar gastric epithelium with a strong cytoplasmic staining [23]. MUC5AC was considered positive if more than 50 % of the gland epithelium showed cytoplasm positive staining. CDX2 was considered negative when a focal loss of staining was seen in more than 10 % of the nuclei of a gland. Foveolar gastric metaplasia was considered in glands with MUC5AC expression and loss of CDX2 staining.

Nuclear positive staining for MLH1 was considered positive, and complete loss of MLH1 expression was defined when all nuclei of dysplastic cells were negative, and considered as a surrogate for *MLH1* promotor hypermethylation. Nuclear immunoreactivity in lymphocytes, normal colonic mucosa or stromal cells served as a positive internal control for *anti*-p53 and *anti*-MLH1.

In lesions with LGD and high-grade dysplasia (HGD), IHC evaluation was performed separately in each dysplastic area for all markers.

2.3. Statistical analysis

Analysis was carried out using SSPS software version 26.0 (SPSS, Chicago, IL, USA). The $\chi 2$ test was used to analyze the association between qualitative variables, whereas the Fisher's exact test and the Student's t-test or the Mann-Whitney test were used for quantitative variables. A $p < 0.05$ was considered statistically significant.

3. Results

3.1. Patients and specimens

Thirty-three colectomy specimens were retrospectively reviewed, 9 (27 %) with CD and 24 (73 %) with UC, from 28 (85 %) men and 5 (15 %) women, aged between 30 and 85 years-old (mean 62.6 years-old). Duration of IBD ranged from 1 to 34 years (mean 14.8 years). In 4 (12.1 %) cases the diagnosis of IBD was made on the colectomy specimen. Acute inflammation was present in 22 (67 %) colectomies. Most of the dysplastic lesions were found in colectomies affected by UC. Twenty-one colectomies (64 %) showed only nonconventional dysplasia, and 7 (21 %) presented only conventional dysplasia. In 5 (15 %) colectomies, 4 (80 %) corresponding to UC, nonconventional and conventional dysplasia occurred simultaneously. Thirteen of the 21 (13/21, 62 %) colectomies with only nonconventional dysplasia had multiple lesions located both in the same and in different sections of the colon. Adenocarcinoma was present in 20 (61 %) specimens. (Table 1).

3.1.1. Nonconventional dysplasia

Sixty-one nonconventional dysplasias were identified, being more frequent in UC (51/61, 84 %), found either alone 36 (59 %), or simultaneously with conventional dysplasia 25 (41 %). In UC a trend was observed between the number of nonconventional dysplasia in relation to disease duration, which was not as evident in CD. The distribution of nonconventional dysplasia according to the location of inflammation was statistically significant ($p = 0.000$). In CD, most of the nonconventional dysplasia were found in the right colon (4/10, 40 %), while in UC they were in the rectum (17/51, 33.4 %) ($p = 0.040$) (Table 2).

The most frequent nonconventional dysplasia were hypermucinous 14 (23 %), goblet cell depleted 12 (19.7 %), and serrated lesion NOS 9 (14.8 %), found mostly in mucosa with active inflammation, especially in UC (Table 2). Histological examples of each nonconventional dysplasia are shown in Fig. 1. The morphologic appearance of the lesions was flat in most nonconventional dysplasia (54 %). Regarding the grade of dysplasia, most nonconventional dysplasia had LGD 31/61 (50.8 %) and all HGD 13/61 (21 %) was observed in UC patients, either alone or with areas of LGD. Nine nonconventional dysplasias (9/61, 14.8 %) presented areas of LGD and HGD, and were distributed as follow: 2/4 (50 %) traditional serrated adenoma-like, 3/7 (43 %) serrated lesion NOS, 3/7 (43 %) sessile serrated lesion-like, and 1/12 (8 %) goblet cell depleted dysplasia. No histological features of dysplasia were found in 17/61 (27.9 %) lesions, corresponding to 10/14 (71 %) hypermucinous dysplasia, 4/7 (57 %) serrated epithelial change, and 3/9 (33 %) serrated lesion NOS (Table 3). Twenty (33 %) nonconventional dysplasias were found concomitant with adenocarcinoma, 9 (15 %) on the same side of the colon, being mostly goblet cell depleted dysplasia (4/12, 33 %), traditional serrated adenoma-like (1/4, 25 %), and hypermucinous dysplasia (3/14, 21 %); and 5 (8.2 %) were found adjacent to the neoplasm, being 2/14 (14 %) hypermucinous dysplasia, 1/7 (14 %) serrated epithelial change, 1/7 (14 %) sessile serrated lesion-like and 1/12 (8 %) goblet cell depleted dysplasia.

3.1.2. Conventional dysplasia

Fifteen conventional dysplasias were identified, 5 (33.3 %) of them simultaneously with nonconventional dysplasia. Seven colectomies showed exclusively conventional dysplasia, being 5 UC and 2 CD. One of the CD specimens had four tubular adenoma-like lesions and the other had only one tubular adenoma-like. Each of the 5 UC colectomies had one tubular adenoma-like.

A statistically significant relation was found between the distribution of conventional dysplasia and the location of inflammation ($p = 0.003$). However, unlike what was observed in nonconventional dysplasia, the relationship between the location of conventional dysplasia with respect to type of IBD was not statistically significant (0.144) (Table 2).

Conventional dysplasia lesions mostly appeared in UC, in specimens with quiescent activity (67 %) and with adenocarcinoma (80 %). Of the 15 conventional dysplasia, 14 (93 %) were tubular adenoma-like with LGD and 1 (7 %) was a tubulovillous adenoma-like with LGD and HGD (Table 2).

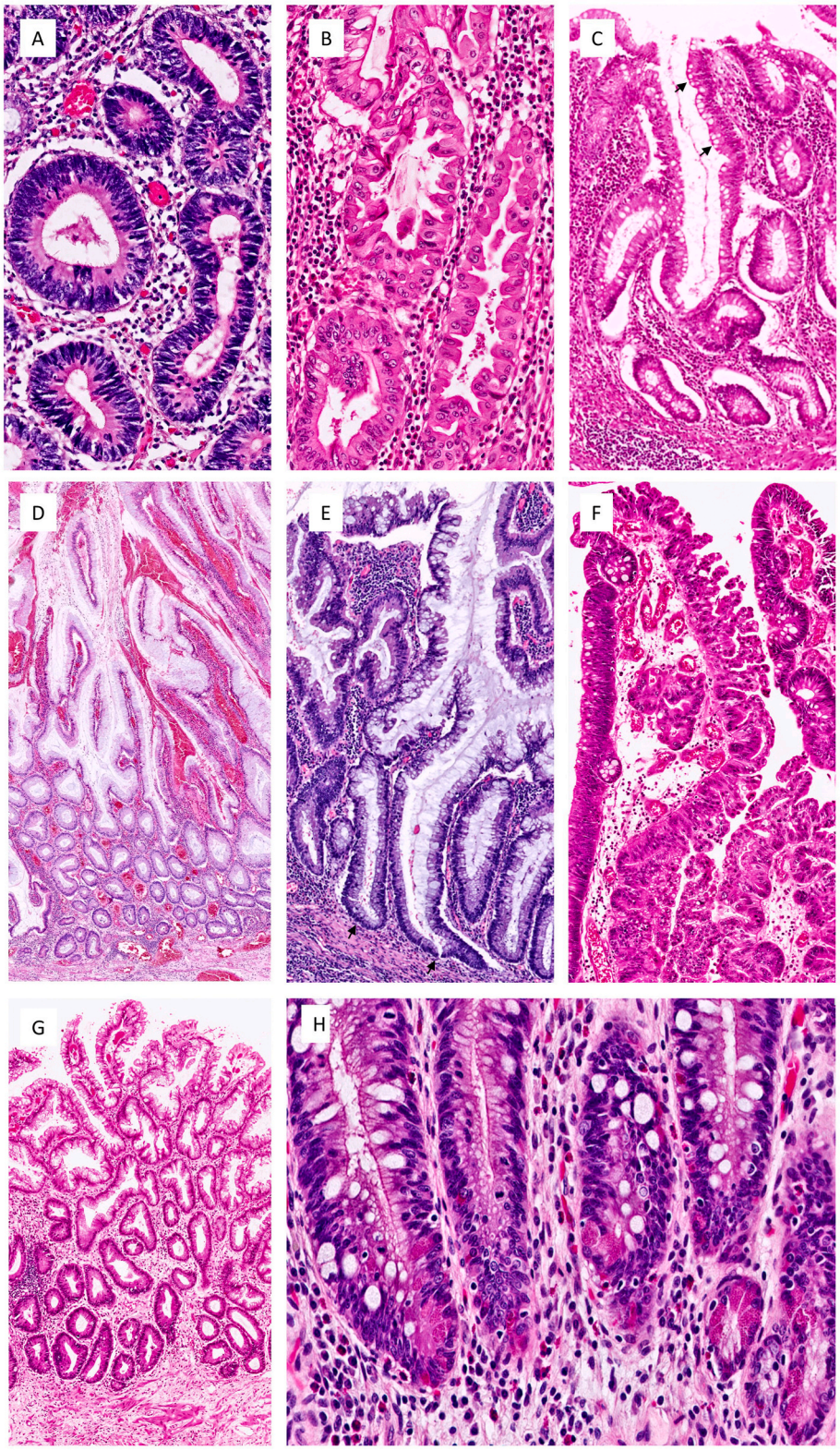

Fig. 1. Histological types of nonconventional dysplasia. Goblet cell deficient dysplasia with unequivocal dysplastic crypts with absence of goblet cells (A). Crypt cell atypia/dysplasia characterized by cells with round-to-oval with non-stratified nuclei (B). Serrated epithelial change with a markedly distorted architecture in which the crypts, some with mild serration (arrows), have lost orientation and were no longer aligned perpendicularly with the muscularis mucosae. Note the chronic inflammation on the lower left side (C). Hypermucinous dysplasia as tubulovillous lesion with prominent mucinous differentiation (D). Sessile serrated lesion-like showing crypts with prominent serrations, dilatations on the base and horizontal growth along the muscularis mucosae (arrows) (E). Traditional serrated adenoma-like with LGD, showing slit-like serration with tall columnar cells with intensely eosinophilic cytoplasm and ectopic crypts formation (F). Serrated lesion NOS, serrated lesion without definite features of traditional serrated adenoma or sessile serrated lesion (G). Dysplasia with increased Paneth cell differentiation showing dysplastic crypts with hyperchromatic nuclei, reduced goblet cells and increased Paneth cell differentiation affecting more than two contiguous crypts (H).

Table 3
MUC5AC, CDX2, p53 and MLH1 IHC expression according to dysplasia type and grade.

	MUC5AC			CDX2			p53			MLH1			
							wt pattern	Mutated pattern					
	Positive	Negative	p value	Positive	Negative	p value		Overexpression pattern	Null pattern	p value	Positive	Partial loss	Complete loss
Nonconventional dysplasia			0.006			0.064				0.003			
HM (n = 14)													
ND = 10	9	1		3	7		9	0	1		0	10	0
LGD = 3	3	0		1	2		1	1	1		0	3	0
HGD = 1	1	0		0	1		0	0	1		0	1	0
GCD (n = 13)													
ND = 0	0	0		0	0		0	0	0		0	0	0
LGD = 10	6	4		7	3		1	4	5		0	10	0
HGD = 3	0	3		3	0		0	1	2		0	3	0
SL NOS (n = 12)													
ND = 3	3	0		0	3		3	0	0		0	3	0
LGD = 6	4	2		4	2		5	0	1		0	6	0
HGD = 3	1	2		2	1		0	1	2		0	3	0
CCA/D (n = 7)													
LGD = 6	5	1		2	4		1	3	2		0	6	0
HGD = 1	0	1		1	0		0	0	1		0	1	0
SEC (n = 7)													
ND = 4	3	1		2	2		4	0	0		0	4	0
LGD = 3	3	0		2	1		3	0	0		0	3	0
SSL-like (n = 10)													
LGD = 7	7	0		2	5		7	0	0		0	7	0
HGD = 3	3	0		1	2		3	0	0		0	3	0
TSA-like (n = 6)													
LGD = 4	3	1		4	0		3	1	0		0	4	0
HGD = 2	0	2		2	0		0	2	0		0	2	0
DPD (n = 1)													
LGD = 1	0	1		1	0		1	0	0		0	1	0
Conventional dysplasia			0.025			0.175							
TA-like (n = 14)													
LGD = 14	1	13		9	5		14	0	0		5	9	0
TVA-like (n = 2)													
LGD = 1	1	0		0	1		1	0	0		0	1	0
HGD = 1	1	0		0	1		1	0	0		0	1	0

Abbreviations: HM, hypermucinous; GCD, goblet cell deficient; SL NOS, serrated lesion not otherwise specified; CCA/D, crypt cell atypia/dysplasia; SEC, serrated epithelial change; SSL-like, sessile serrated lesion-like; TSA-like, traditional serrated adenoma-like; DPD, dysplasia with increased Paneth cell differentiation; TA-like, tubular adenoma-like; TVA-like, tubulovillous adenoma-like; LGD, low-grade dysplasia; HGD, high-grade dysplasia; ND, no dysplasia.

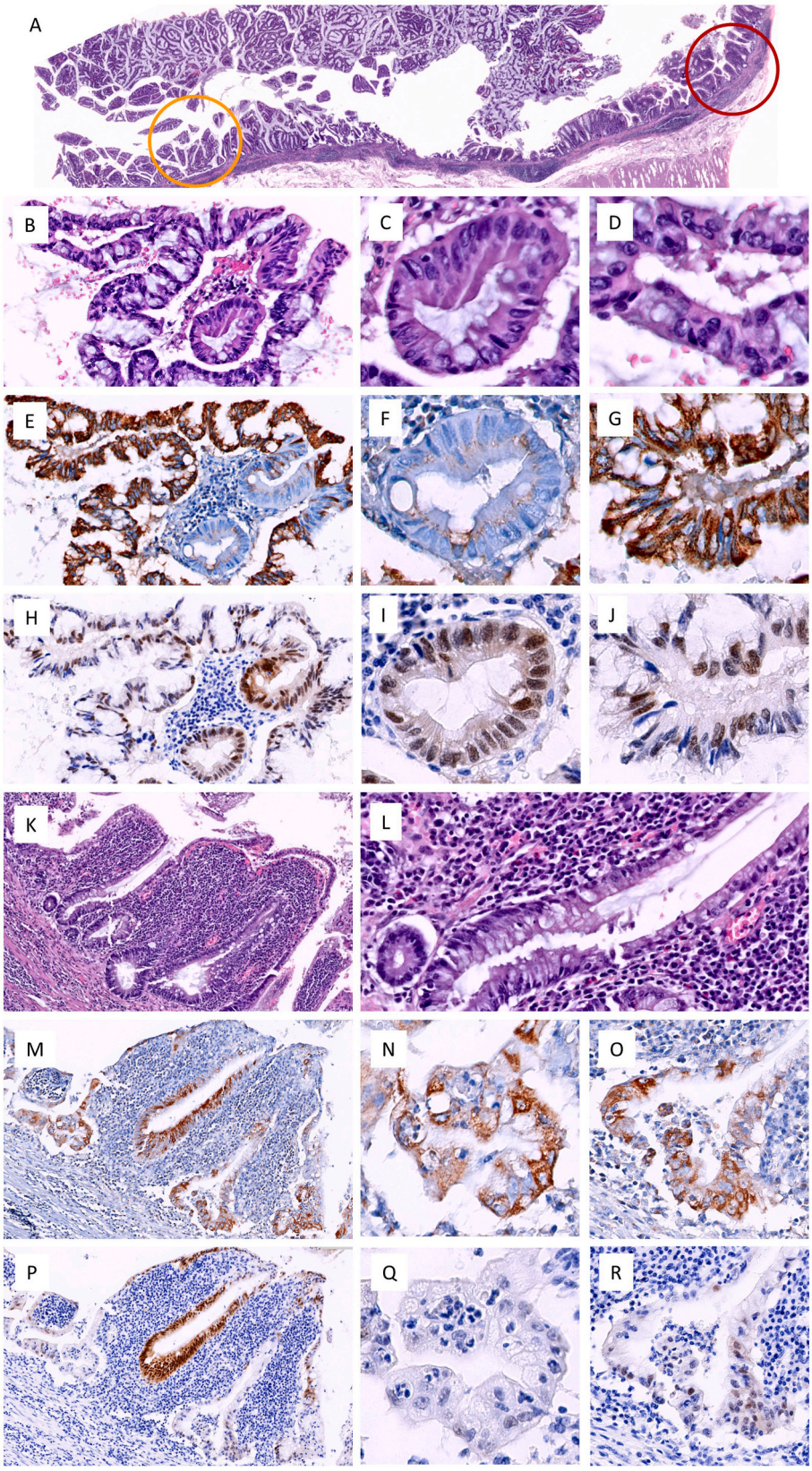

(caption on next page)

Fig. 2. Illustrations of a sessile serrated lesion-like and the adjacent mucosa with MUC5AC and CDX2 IHC. Low power image of a sessile serrated lesion-like (yellow circle) and inflammatory changes in the adjacent mucosa (red circle) (A). Serrated epithelium with LGD containing a gland with HGD with eosinophilic cytoplasms, enlarged nuclei and loss of goblet cells (B). Gland with HGD magnified (C) and epithelia with LGD magnified (D). MUC5AC IHC of the previous lesion (E) showing loss of staining in HGD gland (F) and expression in the epithelium with LGD (G). CDX2 immunostaining in the same lesion (H) with positive staining in the HGD gland (I) and negative or less intensity of the staining in the cells of serrated epithelium with LGD (J). Mucosa with acute and chronic inflammation, erosion, reactive changes and crypt atrophy (K), re-epithelialized epithelium (L) and marked MUC5AC expression (M) with intense staining in the same crypts with acute inflammation (magnified in N and O). CDX2 immunostaining in the same inflamed mucosa (P) with loss of staining in the same crypts with acute inflammation and MUC5AC expression (magnified in Q and R). (For interpretation of the references to color in this figure legend, the reader is referred to the Web version of this article.)

3.1.3. *Adjacent mucosa to the dysplastic lesions*

Presence of colon mucosa was detected more frequently adjacent to conventional dysplasia (80 %, 12/15) than to nonconventional dysplasia (67 %, 41/61). Acute inflammation was seen in only 12 (29 %) cases, all in relation to nonconventional dysplasia; chronic inflammation/changes also occurred more frequently with nonconventional dysplasia (54 % vs 17 %), while normal mucosa was seen more frequently with conventional dysplasia (83 % vs 17 %) (Table 2).

3.2. *Immunohistochemistry*

3.2.1. *Immunohistochemistry in nonconventional dysplasia*

Once the precursor lesions were identified, we used MUC5AC, a well-recognized marker of the foveolar gastric epithelium, to distinguish gastric metaplasia [23]. MUC5AC expression was mostly observed in hypermucinous dysplasia, serrated epithelial change, and serrated lesion NOS without dysplasia (15/17, 88 %). Interestingly, the MUC5AC immunoexpression level decreased with the increase of the grade of dysplasia, being 78 % (31/40) in LGD, and 39 % (5/13) in HGD ($p = 0.006$) (Table 3 and Fig. 2E, F, 2G, 3B, 3F, 3J). Dysplasia with increased Paneth cell differentiation was the only nonconventional dysplasia without MUC5AC expression.

Considering that the loss of CDX2 in the colon is associated with the presence of gastric epithelium, we next analyzed CDX2 expression in the same IBD series. Lack of CDX2 was detected in 12/17 (71 %) lesions without dysplasia, in 17/40 (43 %) LGD and in 4/13 (31 %) HGD ($p = 0.064$) (Table 3 and Fig. 2H, I, 2J, 3C). CDX2 was partially lost or showed less intensity in glands with high expression of MUC5AC ($p < 0.001$) (Table 4).

To investigate the role of gastric metaplasia as a precursor of CAC, we evaluated p53 expression as a surrogate of *TP53* mutation, considering that dysregulation of p53 in one of the most frequent events in this carcinogenesis pathway. The p53-mut pattern (overexpression or null) was observed in 10/13 (77 %) HGD and in 18/40 (45 %) LGD, in contrast to the presence of focal nuclear positivity in almost all the nonconventional dysplasia without dysplasia (16/17, 94 %) ($p < 0.001$) (Table 3 and Fig. 3D, G, 3K).

Finally, to unmask the role of microsatellite instability, we evaluated MLH1 expression as a surrogate for the presence of *MHL1* promoter hypermethylation. We did not find complete loss of nuclear expression in any nonconventional dysplasia, but rather a focal loss of nuclear staining of irregular distribution was observed (Table 3 and Fig. 3H, L).

Once we had determined the expression of the markers in all nonconventional dysplasias, we next assessed the association between MUC5AC and either CDX2 and p53 expression. MUC5AC positivity was associated with the loss of CDX2 expression ($p < 0.001$) (Table 4). Gastric metaplasia was identified in 32 (46 %) nonconventional dysplastic lesions, especially in hypermucinous dysplasia and sessile serrated lesion-like ($p = 0.034$) (Table 5). Regarding to p53 and MUC5AC expression, MUC5AC positive lesions showed mostly a p53-wt pattern (34/51, 67 %), whereas those lacking MUC5AC exhibited mainly a p53-mut pattern (12/19, 63 %) ($p = 0.031$) (Table 4).

3.2.2. *Immunohistochemistry in conventional dysplasia*

MUC5AC was expressed in one (7 %) tubular adenoma-like with LGD and in the tubulovillous adenoma-like (100 %) in areas of LGD and HGD (Table 3 and Fig. 3N). CDX2 was lost in 5 (71 %) of the tubular adenoma-like with LGD and in the tubulovillous-like (100 %), in both LGD and HGD. Gastric metaplasia was identified in one (7 %) tubular adenoma-like with LGD and in the tubulovillous-like (100 %) in areas of LGD and HGD ($p = 0.1875$).

All conventional dysplasia showed a p53-wt pattern (Table 3 and Fig. 3O), 5 tubular adenoma-like retained MLH1 staining and the remaining 9 tubular adenoma-like and the tubulovillous adenoma-like showed partial loss of MLH1 expression (Table 3 and Fig. 3P).

3.2.3. *Immunohistochemistry in adjacent mucosa to the dysplastic lesions*

In mucosa with acute or chronic inflammation, MUC5AC staining was observed at superficial epithelium lining granulation tissue, and in irregular crypts with nuclear stratification and loss of goblet cells (Fig. 2M, N, 2O), whereas CDX2 showed conserved or less intense nuclear expression in the same areas (Fig. 2P, Q, 2 R) as corresponds to the definition of foveolar gastric metaplasia. Gastric metaplasia was identified in the adjacent mucosa of 24 (24/41, 59 %) nonconventional dysplasia, 21 (21/36, 58 %) with UC and 3 (3/5, 60 %) with CD, 8 (8/24, 33.3 %) with active inflammation, 14 (14/24, 58.3 %), chronic changes, and in 2 (2/24, 8.3 %) normal mucosa. No gastric metaplasia was identified in the 12 colon mucosa adjacent to conventional dysplasias (Table 2). A p53-wt pattern was identified in all adjacent mucosa, while MLH1 staining was lost in the superficial epithelium of normal mucosa, as well as in those with active inflammation or chronic changes.

4. Discussion

The aim of this study was to explore the presence of gastric metaplasia and its relationship with dysplasia in a series of nonconventional and conventional dysplastic lesions identified retrospectively from IBD colectomies.

We identified differences in the distribution of both types of dysplasia. While as described in other studies, nonconventional dysplasias were more frequently located in colectomies with acute inflammation, following the characteristic distribution of inflammation according to the type of IBD [24], and observed in specimens without adenocarcinoma, conventional dysplasias were more frequently found in specimens with quiescent activity, unrelated to the inflammation distribution in the colon according to the type of IBD, and with concomitant adenocarcinoma. In contrast to our findings, other authors have found nonconventional dysplasia more frequently associated with advanced neoplasms [19]. However, some of the early precursors such as hypermucinous dysplasia or serrated epithelial were observed

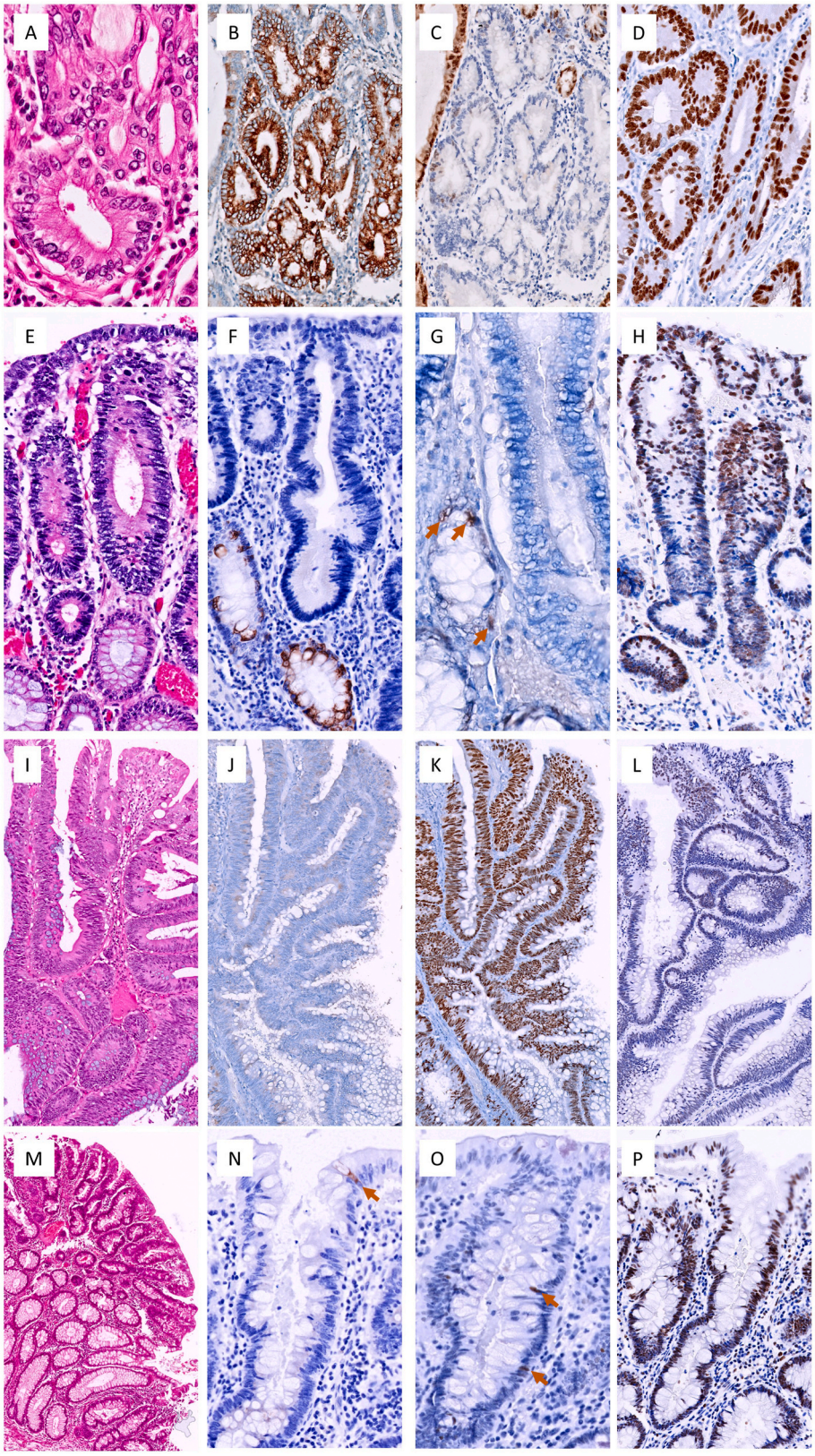

Fig. 3. Examples of IHC in nonconventional and conventional dysplasias. Crypt cell atypia/dysplasia (A) with intense and diffuse cytoplasmic expression of MUC5AC (B), loss of CDX2 (C) and p53-mut pattern (overexpression) (D). Goblet cell depleted dysplasia (E) with loss of MUC5AC (note the positive cytoplasmic staining in adjacent normal glands) (F), p53-mut pattern (null pattern) with positive scattered nuclei in normal glands (arrows) as internal positive control (G) and partial loss of MLH1 expression (H). Traditional serrated adenoma-like (I) without MUC5AC expression (J), p53-mut pattern (overexpression) (K) and partial loss of MLH1 expression (L). Tubular adenoma-like (M) with MUC5AC negative with presence of a single positive cell (arrow) in the surface epithelium (N), p53-wt pattern with scattered positive nuclei (arrows) (O) and MLH1 expression (P).

Table 4
Relation between MUC5AC expression with CDX2 and p53 staining in nonconventional dysplasias.

		MUC5AC			p value
		Positive (%)	Negative (%)	Total (%)	
CDX2	Positive	19 (37)	18 (95)	37 (53)	<0.001
	Negative	32 (63)	1 (5)	33 (47)	
Total		51 (73)	19 (27)	70 (100)	
p53	wt-pattern	34 (67)	7 (37)	41 (59)	0.031
	mut-pattern	17 (33)	12 (63)	29 (41)	
Total		51 (73)	19 (27)	70 (100)	

adjacent to neoplasms, thus confirming the precursor status of these early lesions [7]. No relation was observed in both types of dysplasia with the duration of IBD although there was a trend between UC patients and nonconventional dysplasia.

We found 61 nonconventional dysplastic lesions in 33 IBD specimens. Given the retrospective nature of the studies describing nonconventional dysplasia, the number and type of nonconventional dysplasia identified is highly variable. The number of lesions identified depends directly on the sampling of colectomies and the expertise of the pathologist, since many of them are flat lesions, invisible to macroscopic inspection, and different types are often found in the same specimen [11,17–19,25,27]. Multiple nonconventional dysplasia was present in 13 patients, located on the same and different sides of the colon, as other authors have reported [11,18], while only one patient had multiple conventional dysplastic lesions on the same side of the colon.

The presence of foveolar gastric metaplasia was assessed by the immunoexpression of MUC5AC and loss of CDX2 in the same gland. We observed gastric metaplasia in the superficial epithelia of colon mucosa re-epithelializing granulation tissue, as well as in areas of mucosa with chronic changes, confirming our previous observations about the appearance of gastric metaplasia as an adaptive mechanism to inflammatory damage [21]. In addition, gastric metaplasia was identified mainly in nonconventional dysplasia and its adjacent mucosa with chronic changes in colectomies with UC. We detected gastric metaplasia in all types of nonconventional dysplasia, except for dysplasia with increased Paneth cell differentiation, located in a quiescent UC in the rectosigmoid colon. Considering that crypts with Paneth cells characterize intestinal metaplasia and help identify long-standing IBD when found in the left colon, the absence of gastric metaplasia observed supports its intestinal origin. Gastric metaplasia was mostly observed in nonconventional dysplasia without dysplasia such as hypermucinous dysplasia and in sessile serrated lesion-like but also in crypt cell atypia/dysplasia characterized by dysplastic features. As for conventional dysplasia, gastric metaplasia was identified less frequently than in nonconventional dysplasia (19 % vs. 46 %) and was not detected in any adjacent mucosa, suggesting that gastric metaplasia is not the substrate of origin for conventional dysplasia.

In our study, there was a strong significant association between MUC5AC expression and partial loss of CDX2 supporting the foveolar gastric metaplasia condition. Loss of colonic markers, SATB2 and CDX2, was previously reported by Ma et al. identifying loss of SATB2 in dysplasia and IBD-associated CRC, but not in sporadic patients [28,29]. However, loss of colonic markers was not associated in their studies with the presence of gastric metaplasia.

We observed a progressive decrease in MUC5AC expression with the appearance and increase of the degree of dysplasia. *TP53* gene is the most frequently involved in the early pathway of IBD "inflamed-dysplasia-carcinoma" sequence [7,30,31]. The p53-mut pattern of immunoexpression was identified more frequently in HGD nonconventional dysplasia lacking MUC5AC. Importantly, the fact that MUC5AC expression showed a p53-wt pattern supports that gastric metaplasia precedes the appearance of *TP53* mutations. Expression changes in MUC5AC and p53 reflect the molecular alterations that transform the metaplastic epithelium into dysplastic. Our results support a role for *TP53* in the earliest events of the CAC pathway. We observed altered p53 expression in both low-risk and high-risk nonconventional dysplasia, with increasing rates in higher-grade dysplasia but not in adjacent colonic mucosal or in non-dysplastic nonconventional dysplasia. However, *TP53* mutations, missense and nonsense, had been reported in serrated epithelial change without dysplasia using a NGS approach [7]. The fact that these mutations may be subclonal and the lack of a perfect correlation between the presence of *TP53* mutations and p53 expression could explain the observed discordances [22].

Regarding microsatellite instability, we identified a lack of MLH1 expression in the surface epithelium in both normal mucosa and mucosa with active inflammation or chronic changes. The lack of MLH1 staining in the more mature colon epithelium could be the expression of inactivation of mismatch repair genes in nonproliferating cells. Furthermore, our results agree with previous reports showing the absence of a relevant role of mismatch repair genes in DNA repair phenomena occurring in IBD colonic mucosa [32,33].

Recently, we have shown that CRC characterized by lack of p53 alterations, presence of MUC5AC expression, and complete loss of MLH1 expression appears in IBD probably following the serrated pathway [21]. Although we have demonstrated the presence of foveolar gastric metaplasia in most nonconventional dysplasia, we have not seen a complete loss of MLH1 in any of them that would allow us to identify the precursor lesions of CRC of the serrated pathway. The methylation changes that occur in precursor lesions affect different genes in a non-random manner [34,26]. In sessile serrated lesion, complete loss of MLH1 expression correlates with a threshold for promoter methylation and coincides with the onset of dysplasia [34]. The presence of partial loss of MLH1 staining could be the expression of MLH1 hypermethylation heterogeneity that occurs in both types of precursor lesions [26].

Finally, the pattern of MUC5AC and CDX2 expression observed in conventional dysplasia, especially in tubulovillous adenoma-like, favors the diagnosis of serrated lesions, illustrating the morphological overlap that occurs between both types of lesions [35].

In summary, our results support that foveolar gastric metaplasia appears in IBD colon mucosa as an adaptive mechanism to chronic inflammatory damage, and is the substrate of most nonconventional dysplasia prior to the appearance of *TP53* alterations and is the initial event of CAC and serrated pathway CRC appearing in IBD.

Table 5
Relation of the presence of gastric metaplasia according to the type of nonconventional dysplasias.

Gastric metaplasia	Type of nonconventional dysplasia								Total	p value
	HM	GCD	SL NOS	CCA/D	SEC	SSL-like	TSA-like	DPD		
No	4 (29)	10 (77)	7 (58)	3 (43)	4 (57)	3 (30)	6 (100)	1 (100)	38 (54)	0.034
Yes	10 (71)	3 (23)	5 (42)	4 (57)	3 (43)	7 (70)	0	0	32 (46)	

Abbreviations: HM, hypermucinous; GCD, goblet cell deficient; SL NOS, serrated lesion not otherwise specified; CCA/D, crypt cell atypia/dysplasia; SEC, serrated epithelial change; SSL-like, sessile serrated lesion like; TSA-like, traditional serrated adenoma like; DPD, dysplasia with increased Paneth cell differentiation.

Funding

This work was supported by Roche, Switzerland (activity code: SP210830002).

Ethics approval/consent to participate

This study has been approved by the ethics committee of the Hospital Universitari General de Catalunya (2020/139-APA-HUGC-HUSC-HQV) as well as by the respective ethics committees of the participating centers.

Author contribution statement

M.G., M.C. and E.M., conceptualization, data curation, formal analysis, methodology, investigation; M.G., original draft; M.C. and E.M., writing; E.M., review & editing and funding acquisition; I.A., J.A.V., M. J.F.-A., V·F·C., J.T., I.J., R.F.-V., C.M.-C., C.A.G., C.Z., data curation; M. T.F.-F. and M.E., resources. All authors read and approved the final paper.

Data availability statement

The datasets generated during and/or analyzed during the current study are available from the corresponding author on reasonable request.

Declaration of competing interest

The authors declare no competing financial interests.

Acknowledgements

We want to particularly acknowledge the patients and the technical staff of the Hospital Universitari General de Catalunya-Grupo Quironsalud and Patologia Integrada, S.L. Work technically supported by Xarxa de Bancs de Tumors de Catalunya sponsored by Pla Director d'Oncologia de Catalunya (XBTC).

References

[1] Lutgens MW, van Oijen MG, van der Heijden GJ, et al. Declining risk of colorectal cancer in inflammatory bowel disease: an updated meta-analysis of population-based cohort studies. Inflamm Bowel Dis 2013;19:789–99. https://doi.org/10.1097/MIB.0b013e31828029c0.

[2] Jess T, Gamborg M, Matzen P, et al. Increased risk of intestinal cancer in Crohn's disease: a meta-analysis of population-based cohort studies. Am J Gastroenterol 2005;100:2724–9. https://doi.org/10.1111/j.1572-0241.2005.00287.x.

[3] Mattar MC, Lough D, Pishvaian MJ, et al. Current management of inflammatory bowel disease and colorectal cancer. Gastrointest Cancer Res 2011;4:53–61.

[4] Linson EA, Hanauer SB. Epidemiology of colorectal cancer in inflammatory bowel disease - the evolving landscape. Curr Gastroenterol Rep 2021;23:16. https://doi.org/10.1007/s11894-021-00816-3.

[5] Da Cunha T, Vaziri H, Wu GY. Primary sclerosing cholangitis and inflammatory bowel disease: a review. J Clin Transl Hepatol 2022;10:531–42. https://doi.org/10.14218/JCTH.2021.00344.

[6] Galandiuk S, Rodriguez-Justo M, Jeffery R, et al. Field cancerization in the intestinal epithelium of patients with Crohn's ileocolitis. Gastroenterology 2012;142:855–64. https://doi.org/10.1053/j.gastro.2011.12.004.

[7] Singhi AD, Waters KM, Makhoul EP, et al. Targeted next-generation sequencing supports serrated epithelial change as an early precursor to inflammatory bowel disease-associated colorectal neoplasia. Hum Pathol 2021;112:9–19. https://doi.org/10.1016/j.humpath.2021.03.002.

[8] Schlemper RJ, Riddell RH, Kato Y, et al. The Vienna classification of gastrointestinal epithelial neoplasia. Gut 2000;47:251–5. https://doi.org/10.1136/gut.47.2.251.9.

[9] Riddell RH, Goldman H, Ransohoff DF, et al. Dysplasia in inflammatory bowel disease: standardized classification with provisional clinical applications. Hum Pathol 1983;14:931–68. https://doi.org/10.1016/S0046-8177(83)80175-0.

[10] Harpaz N, Goldblum JR, Shepherd N, et al. Novel classification of dysplasia in IBD. Mod Pathol 2017;30:174A. https://doi.org/10.1007/978-3-030-51268-2_6.

[11] Choi WT, Yozu M, Miller GC, et al. Nonconventional dysplasia in patients with inflammatory bowel disease and colorectal carcinoma: a multicenter clinicopathologic study. Mod Pathol 2020;33:933–43. https://doi.org/10.1038/s41379-019-0419-1.

[12] Wen KW, Umetsu SE, Goldblum JR, et al. DNA flow cytometric and interobserver study of crypt cell atypia in inflammatory bowel disease. Histopathology 2019;75:578–88. https://doi.org/10.1111/his.13923.

[13] Gui X, Köbel M, Ferraz JGP, et al. Newly recognized non-adenomatous lesions associated with enteric carcinomas in inflammatory bowel disease - report of six rare and unique cases. Ann Diagn Pathol 2020;44:151455. https://doi.org/10.1016/j.anndiagpath.2019.151455.

[14] Waters KM, Singhi AD, Montgomery EA. Exploring the spectrum of serrated epithelium encountered in inflammatory bowel disease. Hum Pathol 2023;132:126–34. https://doi.org/10.1016/j.humpath.2022.06.018.

[15] Johnson DH, Taylor WR, Aboelsoud MM, et al. DNA Methylation and mutation of small colonic neoplasms in ulcerative colitis and Crohn's colitis: implications for surveillance. Inflamm Bowel Dis 2016;22:1559–67. https://doi.org/10.1097/MIB.0000000000000795.

[16] Choi WT, Wen KW, Rabinovitch PS, et al. DNA content analysis of colorectal serrated lesions detects an aneuploid subset of inflammatory bowel disease-associated serrated epithelial change and traditional serrated adenomas. Histopathology 2018;73:464–72. https://doi.org/10.1111/his.13652.

[17] Kamarádová K, Vošmiková H, Rozkošová K, et al. Non-conventional mucosal lesions (serrated epithelial change, villous hypermucinous change) are frequent in patients with inflammatory bowel disease-results of molecular and immunohistochemical single institutional study. Virchows Arch 2020;476:231–41. https://doi.org/10.1007/s00428-019-02627-4.

[18] Gui X, Köbel M, Ferraz JG, et al. Histological and molecular diversity and heterogeneity of precancerous lesions associated with inflammatory bowel diseases. J Clin Pathol 2020;73:391–402. https://doi.org/10.1136/jclinpath-2019-206247.

[19] Lee H, Rabinovitch PS, Mattis AN, et al. Non-conventional dysplasia in inflammatory bowel disease is more frequently associated with advanced neoplasia and aneuploidy than conventional dysplasia. Histopathology 2021;78:814–30. https://doi.org/10.1111/his.14298.

[20] Chen B, Scurrah CR, McKinley ET, et al. Differential pre-malignant programs and microenvironment chart distinct paths to malignancy in human colorectal polyps. Cell 2021;184:6262–80. https://doi.org/10.1016/j.cell.2021.11.031.

[21] Gené M, Cuatrecasas M, Amat I, et al. Alterations in p53, microsatellite stability and lack of MUC5AC expression as molecular features of colorectal carcinoma associated with inflammatory bowel disease. Int J Mol Sci 2023;24:8655. https://doi.org/10.3390/ijms24108655.

[22] Köbel M, Piskorz AM, Lee S, et al. Optimized p53 immunohistochemistry is an accurate predictor of *TP53* mutation in ovarian carcinoma. J Pathol Clin Res 2016;2:247–58. https://doi.org/10.1002/cjp2.53.

[23] Rico SD, Mahnken M, Büscheck F, et al. MUC5AC Expression in various tumor types and nonneoplastic tissue: a tissue microarray study on 10399 tissue samples. Technol Cancer Res Treat 2021;20:15330338211043328. https://doi.org/10.1177/15330338211043328. Erratum in: Technol Cancer Res Treat. 2022 Jan-Dec;21:15330338221099574.

[24] Nguyen ED, Wang D, Lauwers GY, et al. Increased histologic inflammation is an independent risk factor for nonconventional dysplasia in ulcerative colitis. Histopathology 2022;81:644–52. https://doi.org/10.1111/his.14765.

[25] Zhang R, Lauwers GY, Choi WT. Increased Risk of Non-Conventional and Invisible Dysplasias in patients with primary sclerosing cholangitis and inflammatory bowel disease. J Crohns Colitis 2022;16:1825–34. https://doi.org/10.1093/ecco-jcc/jjac090.

[26] Dhir M, Yachida S, Van Neste L, et al. Sessile serrated adenomas and classical adenomas: an epigenetic perspective on premalignant neoplastic lesions of the gastrointestinal tract. Int J Cancer 2011;129:1889–98. https://doi.org/10.1002/ijc.25847.

[27] Bahceci D, Lauwers GY, Choi WT. Clinicopathologic features of undetected dysplasia found in total colectomy or proctocolectomy specimens of patients with inflammatory bowel disease. Histopathology 2022;81:183–91. https://doi.org/10.1111/his.14673.

[28] Ma C, Olevian D, Miller C. SATB2 and CDX2 are prognostic biomarkers in DNA mismatch repair protein deficient colon cancer. Mod Pathol 2019;32:1217–31. https://doi.org/10.1038/s41379-019-0265-1.

[29] Ma C, Henn P, Miller C, et al. Loss of SATB2 Expression Is a biomarker of inflammatory bowel disease-associated colorectal dysplasia and adenocarcinoma. Am J Surg Pathol 2019;43:1314–22. https://doi.org/10.1097/pas.0000000000001330.

[30] Leedham SJ, Graham TA, Oukrif D, et al. Clonality, founder mutations, and field cancerization in human ulcerative colitis-associated neoplasia. Gastroenterology 2009;136:542–50. https://doi.org/10.1053/j.gastro.2008.10.086.

[31] Robles AI, Traverso G, Zhang M, et al. Whole-exome sequencing analyses of inflammatory bowel disease – associated colorectal cancers. Gastroenterology 2016;150:931–43. https://doi.org/10.1053/j.gastro.2015.12.036.
[32] De Angelis PM, Dorg L, Pham S, et al. DNA repair protein expression and oxidative/nitrosative stress in ulcerative colitis and sporadic colorectal cancer. Anticancer Res 2021;41:3261–70. https://doi.org/10.21873/anticanres.15112.
[33] Cawkwell L, Sutherland F, Murgatroyd H, et al. Defective hMSH2/hMLH1 protein expression is seen infrequently in ulcerative colitis associated colorectal cancers. Gut 2000;46:367–9. https://doi.org/10.1136/gut.46.3.367.
[34] Liu C, Fennell LJ, Bettington ML, et al. DNA methylation changes that precede onset of dysplasia in advanced sessile serrated adenomas. Clin Epigenet 2019;11:90. https://doi.org/10.1186/s13148-019-0691-4.
[35] Cansiz Ersöz C, Kiremitci S, Savas B, et al. Differential diagnosis of traditional serrated adenomas and tubulovillous adenomas: a compartmental morphologic and immunohistochemical analysis. Acta Gastroenterol Belg 2020;83:549–56.